

Role of key amino acids in the transmembrane domain of the Newcastle disease virus fusion protein

Yanan Huang¹, Yaqing Liu¹, Yanguo Li², Ying Liu¹, Chi Zhang¹, Hongling Wen¹, Li Zhao¹, Yanyan Song¹, Liyang Wang^{3,*}, Zhiyu Wang^{1,*}

¹Department of Virology, School of Public Health, Cheeloo College of Medicine, Shandong University, Ji'nan, Shandong, China;

²Department of Health Management and Services, Cangzhou Medical College, Cangzhou, Hebei, China;

³Department of Clinical Laboratory, Qilu Hospital, Cheeloo College of Medicine, Shandong University, Ji'nan, Shandong, China.

SUMMARY Newcastle disease (ND), caused by the Newcastle disease virus (NDV), is transmitted by poultry with severe infectivity and a high fatality rate. The fusion (F) protein on the NDV envelope facilitates the merger of the viral and host cell membranes with the help of the homologous hemagglutinin-neuraminidase protein (HN). The transmembrane (TM) domains of viral fusion proteins are typically required for fusion, but the key amino acids in NDV F TM domains have not been identified. Site-directed mutagenesis was utilized to change the conserved amino acids at 500, 501, 502, 505, 510, 513, 516, 519, and 520 to alanine. It was found that mutants L519 and V520 had an interrupted protein expression, decreased to below 10%, and mutants A500, I505, V513, and V516 had a hypoactive impact on fusion activity, decreased to 85.38%, 67.05%, 55.38% and 51.13% of wt F, respectively. The results indicated that the TM domain plays a vital part in the fusion activity of the NDV F protein.

Keywords NDV, fusion protein, transmembrane domain, cell fusion

1. Introduction

Newcastle disease (ND), caused by the virulent Newcastle disease virus (NDV) and resulting in high mortality in the avian industry, causes devastating economic effects on a wide range of domestic and wild bird production worldwide. Despite current vaccination protocols utilized to quell the disease, the potential for future outbreaks and the hazards of other analogous paramyxoviruses require further study of the entry mechanism. Membrane fusion to process infection is mainly mediated and coordinated by a combination of the homologous hemagglutinin-neuraminidase (HN) protein responsible for receptor binding and a fusion (F) protein undergoing irreversible conformation rearrangement coupling of the energy released with membrane coalition of the virus membrane protein (1).

Before participating in merging, the NDV F protein, initially synthesized as inactive form F₀, requires proteolytically cleavage to become the disulfide bonded F₁ and F₂ active complex form (2). F₁ has two hydrophobic regions, the N-terminal fusion peptide (FP) located at the new N-terminal after cutting, transmembrane (TM) domains, and two heptad repeat (HR) regions, HRA and HRB (Figure 1A). HRA lies at the C-terminal of FP, and HRB is adjacent to the TM

domain (3). Atomic structures of several paramyxovirus F proteins for parainfluenza virus 5 (PIV5), respiratory syncytial virus (RSV), human metapneumovirus (hMPV), Hendra virus (HeV), and Nipah virus (NiV) in the prefusion form and hPIV3, NDV, and RSV in the post-fusion form have been determined by X-ray crystallography. While all of these protein architectures are ectodomains, the C-terminal regions are among the least well-understood (4).

Several studies have shown that the TM domain aids in protein folding, stability and fusion beyond merely anchoring *via* replacement with other fusion protein TM domains. Little is known about the secondary structure of the TM domain of viral fusion proteins. Researchers applied solid-state nuclear magnetic resonance to determine the backbone conformation and oligomeric structure of the TM domain of the PIV5 F protein in lipid bilayers. It was found that the secondary structure of TM domain depends on various membrane compositions (5,6). The TM domain can adopt a transmembrane strand-helix-strand conformation, which causes different curvatures to the two leaflets of the membrane in order to help drive the hemi-fusion to fusion pore transition. In spite of the TM domain conformation depending to a great extent on the lipid composition, the amino acid sequence of the TM domain also exhibits an intrinsic

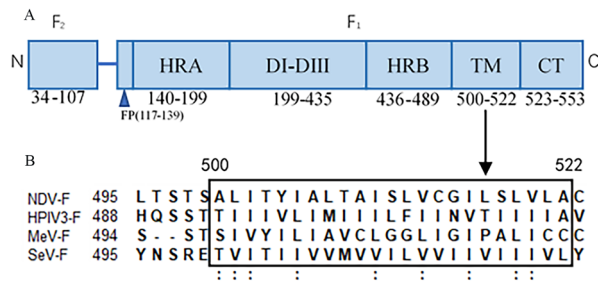


Figure 1. Schematic diagram of the locations of mutations. (A) Domain structure of the NDV F protein. Fusion peptide (FP), heptad repeat region (HR), and structural domains (DI-DIII), transmembrane region (TM), and cytoplasmic tail are shown. **(B)** Identification of the conserved amino acids in the TM domain by sequence alignment using BioEdit software. The asterisk (**) represent similar amino acids in the F protein of NDV, hPIV3, MeV and SeV.

preference for the α -helix or β -chain conformation. Importantly, β -branched residues comprise 30-75% of the TM domain sequences of 10 paramyxoviruses and the human immunodeficiency virus (HIV) (6). Also, the shift of β -branched residues support this notion, revealing that these residue mutations of the TM domain of the Hendra virus F seriously diminished fusion activity (7).

The current experiments demonstrated that the TM domain of paramyxovirus F, such as PIV5, hMPV, and HeV self-associate in a monomer-trimer equilibrium in isolation (8,9). It is very likely that trimeric TM-TM interactions are characteristic of F proteins throughout the paramyxovirus family. They even have similar features with other class I viral fusion proteins including the Ebola virus glycoprotein, influenza virus hemagglutinin, and severe acute respiratory syndrome coronavirus spike protein (10). This is helpful for the development of an antiviral target using the TM-TM interaction to destroy the fusion protein function (11).

Additionally, the presence or absence of certain TM motifs has been implicated in promotion of modulating protein oligomerization and function. This includes central glycine motifs (7,12) (i.e., GXXXG, where X is any amino acid) and a leucine zipper-like (13) (or heptad repeat-like) arrangement of leucine/isoleucine residues. However, the PIV5 F TM L/I zipper does not significantly affect protein expression, but is critical for fusogenic activity, and only affects pre-fusion stability (14). These results suggest that F proteins of paramyxoviruses have inherent sequence requirements for their TM domains, rather than certain interaction motifs. Replacement of the NDV F protein TM domain with Measles virus (MeV), Sendi virus (SeV), and vesicular stomatitis virus (VSV) F proteins lead to proteins with defective fusion activities (15). Upon further investigation, residues L486 and I488 of PIV5 F TM domain are considered to act as a key role in fusion (16). Nevertheless, the key amino acids in the NDV F TM domain have not been identified. These features aroused our interest and in part motivated the present

study. Therefore, we compared the TM domains among several paramyxoviruses (Figure 1B) in order to define the targets for mutagenesis.

2. Materials and Methods

2.1. Strain and plasmids

The strain was *E. coli* DH5 α . Vector pBluescript SK (+) (pBSK⁺) containing NDV-Australia-Victoria HN and F were kindly presented with Professor Iorio. The NDV F gene was cloned and inserted at *Xho* I (668), and the NDV HN gene was inserted between *Xba* I and *Sac* I.

2.2. Cell line and viruses

BHK-21 cells were maintained in Dulbecco modified Eagle medium (DMEM) (Biological Industries (BI), Beit-Haemek, Israel) supplemented with 10% (v/v) fetal bovine serum (FBS) (BI) and 1% (v/v) penicillin/streptomycin (BI). The recombinant vaccinia virus (vTF7-3), a present of Dr. Bernard Moss, provided T7 polymerase for the transient expression system of vaccinia virus-T7 RNA polymerase used to express the wild type (wt) or mutated F protein, while the wt vaccinia virus was used as the control in the content mixing assay.

2.3. Construction of F TMD mutants

The mutants for the NDV F TM domain were constructed by changing interested residues to alanine, which is the chiral amino acid with the shortest side chain and has little influence on the spatial structure of proteins according to the alignment of NDV, hPIV3, MeV, and SeV F TM domains. Using pBSK⁺-F as a template, the mutants were obtained by Gene splicing by overlap extension PCR (SOE PCR) with the assistance of two pairs of reverse-complement primers, mutagenesis oligonucleotide primers and vector oligonucleotide primers (Table 1) (Sangon Biotech Co. Ltd., Shanghai, China) (17). All constructs were sequenced to verify that only the desired mutations had occurred. The recombinant plasmids were transformed into *E. coli* DH5 α for amplification and extracted with the ENZA Plasmid Miniprep Kit (Omega Bio-Tek, Inc., USA) for subsequent experiments.

2.4. Transfection

BHK-21 cells were cultured in 12-well plates at a density of 4×10^5 cells per well before transfection. After 70-80% confluence, the cells were incubated with vTF7-3 (1:50) in serum-free DMEM for 1 h at 37°C in a 5% CO₂ incubator to allow for infection of vTF7-3. Subsequently, the supernatant was removed and the cells were washed with serum-free DMEM,

Table 1. Mutant primer sequences

Name	Sequence (5'-3')
Vector-FP	GGTATTGTCTCATGAGCGGATACA
Vector-RP	TGTATCCGCTCATGAGACAATAACC
A500T-FP	CTGACCAGCACATCTACTCTCATTACCTATATC
A500T-RP	GATATAGGTAATGAGAGTAGATGTGCTGGTCAG
L501A-FP	ACCAGCACATCTGCTGCCATTACCTATATCGCT
L501A-RP	AGCGATATAGGTAATGGCAGCAGATGTGCTGGT
I502A-FP	AGCACATCTGCTCTCGCTACCTATATCGCTTTA
I502A-RP	TAAAGCGATATAGGTAGCGAGAGCAGATGTGCT
I505A-FP	GCTGTCATTACCTATGCGGCTTAACTGCCATA
I505A-RP	TATGGCAGTTAAAGCGGCATAGGTAATGAGAGC
I510A-FP	ATCGCTTTAACTGCCGATCTCTGTTTGGCGGT
I510A-RP	ACCGCAAACAAGAGATGCGGCGAGTTAAAGCGAT
V513A-FP	ACTGCCATATCTCTTGCTTGCGGTATACTTAGT
V513A-RP	ACTAAGTATACCGCAAGCAAGAGATATGGCAGT
I516A-FP	TCTCTTGTTCGGTGCACTTAGTCTGGTTCTA
I516A-RP	TAGAACCAGACTAAGTGCACCGCAAACAAGAGA
L519A-FP	GTTTGGCGGTACTTCTGCTGTTCTAGCATGC
L519A-RP	GCATGCTAGAACAGAGCAAGTATACCGCAAAC
V520A-FP	TGCGGTATACTTAGTGGGTTCTAGCATGCTAC
V520A-RP	GTAGCATGCTAGAACCGCACTAAGTATACCGCA

The 9 amino acids in the TM domain were mutated to A (A500 is mutated to T) by overlapping PCR. *Xba* I digested pBSK⁺-F was used as the template to create one PCR fragment with primers mutations-FP (forward primer) and Vector-RP (reverse primer). The same plasmid digested by *Kpn* I was used as the template to generate the other PCR fragment with primers mutations-RP and Vector-FP. Two PCR products at each mutation point with homologous ends were transformed into DH5 α competent cells to obtain the desired mutants. Mutated sites are underlined in the primer sequences.

and 1 mL complete medium (DMEM with 10% FCS) was added into each well, and then transfected with 4 μ L TurboFectTM Transfection Reagent (Thermo Fisher Scientific, USA) and 4 μ g either wt and mutant F plasmids and/or the wt HN plasmid, the two of which were gently pre-mixed together.

2.5. Indirect immunofluorescent assay (IIFA)

After 36 h transfection, monolayers of BHK-21 cells were fixed with 4% paraformaldehyde for 15 min before washing twice with phosphate-buffered saline (PBS), followed by incubation for 4 h at 4°C with 3% PBSA (in PBS supplemented with bovine serum albumin). Then the cells were incubated with anti-NDV antiserum (ab34402, Abcam, Cambridge, UK, at a 1:1,000 dilution) recognizing the NDV F protein and an Alexa Fluor 488-conjugated goat anti-chicken IgY (H+L) (ab150169, Abcam, diluted 1:10,000) as the secondary antibody. The cells were recorded under a fluorescent microscope (Olympus, Tokyo, Japan) after the secondary antibody was washed twice with PBS.

2.6. Fluorescence-activated cell sorter (FACS) analysis

To quantify the F protein surface expression levels, transfected BHK-21 cells were transferred by PBS configured 0.02% EDTA to a centrifuge, washed twice, and blocked with PBSA for 30 min, followed by

incubation with primary and secondary antibodies, the same as the IIFA. Then, the cells were immobilized with 4% paraformaldehyde and subsequently resuspended in 300 μ L PBSA for analysis with the Flow Cytometer (FACSCelesta, BD, USA).

2.7. Dye transfer assay

R18, a lipolyphilic probe (Invitrogen, California, USA), which was transferred from chicken red blood cells to fuse BHK-21 cells as co-transfected with NDV HN and wt or the mutated F gene, were used to access hemi-fusion of membrane-membrane. At 22 h post-transfection, the R18-labelled RBCs were added to BHK-21 cells in 12-well plates and incubated for 0.5 h on ice. Cells were incubated 1h at 37°C after the unbound RBCs were washed by cold PBS containing 0.1 mM CaCl₂ and 1 mM MgCl₂ (PBS-CM), and then the results of the lipid mixing were photographed under a fluorescent microscope (Olympus).

2.8. Reporter gene assay

Effector cells were co-transfected with the desired F and NDV HN genes with the help of vTF7-3. Target cells infected with the WT vaccinia virus were transfected with 1 μ g of plasmid pG1NT7 β -gal, which encodes β -galactosidase. After 18 h, effector cells were overlaid with target cells (which stably express the T7 polymerase) at an approximate 1:1 ratio at 37°C for 12 h in a 96-well microtiter plate. The cells were then lysed and assayed for β -galactosidase activity according to the β -galactosidase assay kit manufacturer's instructions (Beyotime Biotechnology, Shanghai, China). Values were normalized to samples containing the desired F and NDV HN, with the wild-type levels set at 100% after subtraction of the values for NDV HN alone.

2.9. Syncytium assays

BHK-21 cells seeded into 12-well plates were co-transfected with wt F or mutant F genes along with the NDV HN gene after incubation with the recombinant vaccinia virus 1h earlier at 37°C. Monolayer cells fixed with methanol and stained with Gimasa solution were examined for syncytium formation at 24 h post-transfection using an inverted microscope (Olympus).

2.10. Western Blot

At 36 h post-transfection, the lysate of cells was harvested, pelleted, and loaded in 12% polyacrylamide gels. After electrophoresis, the proteins were transferred from the gels to polyvinylidenedifluoride (PVDF) membranes, blocked with 5% nonfat milk, and incubated with primary and secondary antibody (IRDye 800CW donkey anti-chicken antibody, LI-COR,

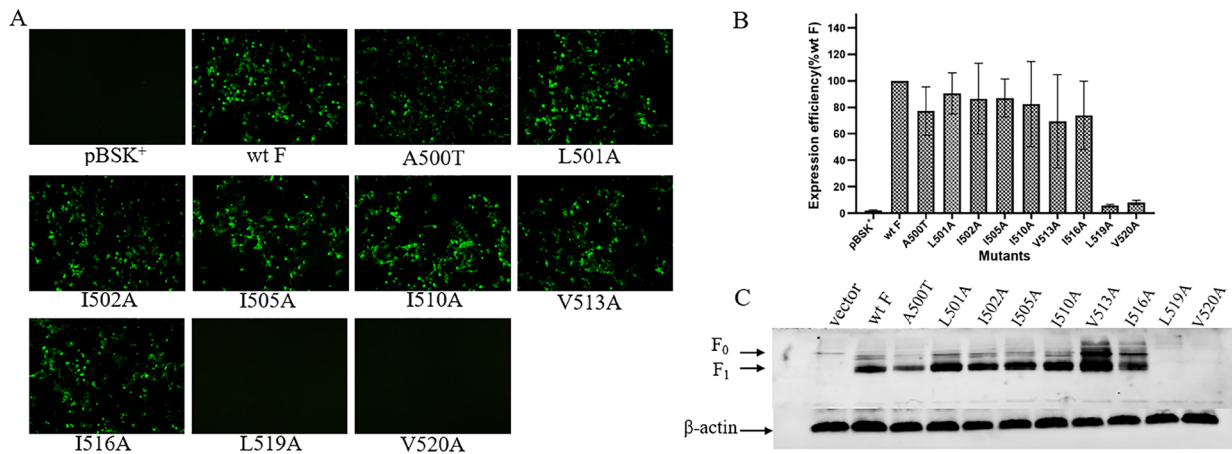


Figure 2. The results of cell surface expression and cleavage activity of wt and mutant F protein. (A) Qualitative results of cell surface expression of mutant F proteins by IIFA. Monolayers of BHK-21 cells transfected with wt or mutant F genes were incubated with anti-NDV antiserum and then with fluorescent-labeled goat anti-chicken antibody. (Magnification: 100 \times). (B) Quantitative detection results of cell surface expression efficiency of mutant F proteins by FACS analysis. Data were normalized to the value obtained with wt F. C: Expression and cleavage of NDV wt F and F mutants transfected without HN. β -actin was used as the internal reference.

Lincoln, Nebraska, USA). Protein bands were scanned and visualized with Odyssey (LI-COR).

2.11. Statistics and data analysis

All results were generated from at least three separate experiments and presented as the mean \pm SD. Statistical analysis was evaluated by the Student's *t* test using SPSS 20.0 with a significance level of $p < 0.05$ (*), $p < 0.01$ (**) and $p < 0.001$ (***), respectively.

3. Results

3.1. Cell surface expression of wt F and its mutants

To explore whether or not these mutated F proteins were expressed at the cell surface, indirect immunofluorescent detection and fluorescent-activated cell sorting were used to qualitatively and quantitatively analyze their protein expressions on the cell surface. As shown in Figure 2A, there were discernable fluorescent signals between most mutants and wt F, except for L519A and V520A, for which signals were barely detected. Similar to FACS analysis, most mutants expressed as much as 70-90% of wt F (Figure 2B).

3.2. Cleavage activity of NDV wt F and mutants

Only by being proteolytically cleaved can the F protein become biologically active, therefore Western Blot was applied to test cleavage activity of NDV wt F and mutants (Figure 2C). The experiment revealed that most mutants were expressed at wt levels on the surface, but mutants L519A and V520A were noncleaved and expressed less than the wt F protein as expected, in agreement with the result of IIFA and FACS. The extent of cleavage of F mirrored the surface expression levels.

3.3. Fusion activity assay for wt F and its mutants

The process of viral membrane fusion involves a series of intermediate steps such as hemifusion (local membrane approach), pore formation, and pore enlargement. In order to analyze the effect of single amino acid substitution of conserved amino acids within the TM domain of NDV F concerning their fusion activity, three types of fusion activity experiments were conducted to measure hemi-fusion, content mixing, and syncytium formation.

First, through the process of membrane fusion, merger of the contacting outer leaflet resulted in hemifusion *via* a stalk intermediate that occurred at an early stage. To address whether or not mutants affect the ability to mediate subsequent content mixing, a R18 dye transfer assay was used to evaluate the extent of the lipophilic probe R18 transferred from RBC membranes to transfected BHK-21 cell membranes. Figure 3A displays representative photomicrographs of the dye transfer experiment. When monolayer cells were mock transfected with F alone, most mutants behaved in a manner similar to that of wt F and HN except for L519A and V520A, but there was a slight decrease in mutants A500T, I505A, V513A, and V516A. These results substantiate the idea that the existence of these mutants does not preclude the lipid mixing stage.

Second, content mixing was measured by using a β -galactosidase reporter gene assay. When two populations of cells were mixed, one co-expressed wt or mutated F along with HN, and the other transfected with the pGINT7 β -gal plasmid and the pGINT7 β -gal gene was activated to synthesize galactoside, which reacted with the substrate galactopyranoside to yield a bright yellow color. The intensity of the reaction results in the shade reflects the extent of cell fusion events. As Figure 3B shows, mutant A500T, L501A, I502A, and I510A

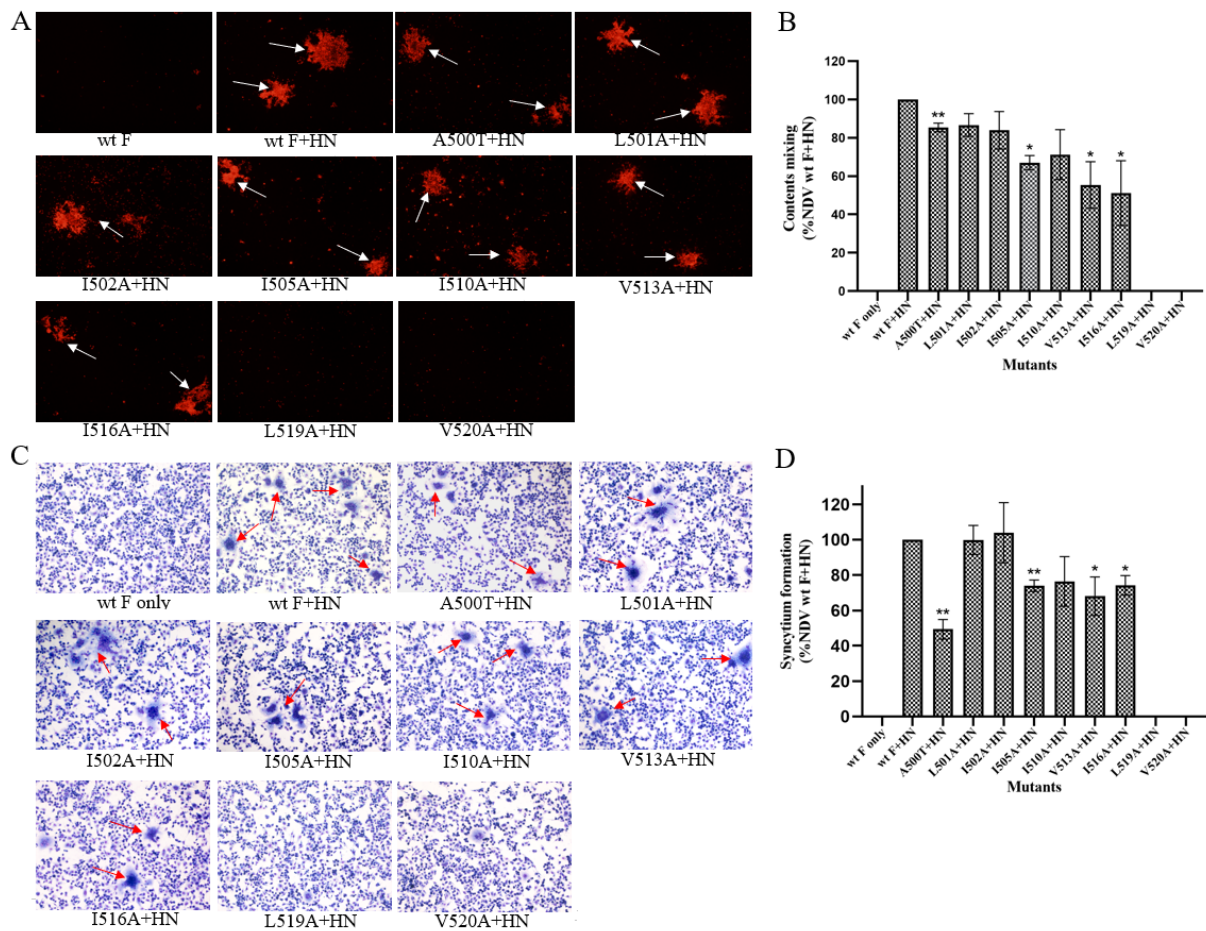


Figure 3. Fusion ability detection of F mutants. (A) Determination of lipid mixing for NDV wt and mutant F proteins (Magnification: 100 \times). Labeled RBCs were added to BHK-21 monolayer in order to observe the extent of lipid mixing. (B) Quantification of content mixing of mutants measured by the reporter gene method. The values were expressed as percentages of positive control co-transfected with wt HN and F. (C) The results of the syncytium formation assay of substitution mutants. The arrows point to the syncytium. (Magnification: 100 \times). (D) Quantitative results of syncytium area. Syncytia size was quantified by measuring the area covered by syncytia using Image Proplus software, referring it to the total area of the field for three random fields.

had 85.38%, 86.69%, 83.92 % and 71.24% of the levels of content mixing of the wt F protein, respectively, with L519A and V520A almost non-existent. The mutants I505A, V513A and V516A had a lower level of content mixing of 67.05%, 55.38% and 51.13% of that of wt F proteins. The preponderance of data indicated that several motifs were able to change content mixing.

Lastly, a syncytium fusion assay (Figures 3C and 3D) was used to determine whether the TM domain mutants affected the F protein function. Using cells expressing wt F only as mock, the cells that co-expressed wt or mutated F together with HN were imaged to visualize syncytia. That is, membrane fusion between neighboring cells leads to the formation of giant multinucleated cells. There was no significant difference in the number and size of syncytia formed by L501A and I502A, 100% and 104% as fusogenic as the wt F protein, respectively, and I510A was moderately fusogenic, while the mutants L519A and V520A were fusion dead. The numbers of fused spots by the mutants A500T, I505A, V513A, and V516A in the presence of the HN protein were fewer in number than those produced by wt F and HN

proteins (only 50-75% of the wt F level). These data demonstrated that individual residue replacement has various phenotypes with none to significant effects on syncytium formation.

4. Discussion

The fusion protein is generally envisioned to exist on the mature viral surface in a 'native' fusion-competent state, followed by fusion-associated conformational fold-back steps, during which the fusion subunit converts to a compact trimer-of-hairpins resembling a ball on a stick. In the prefusion structure (18), the spherical head consists of domains I through III (DI-DIII), HRA is located on the flanks of them, and DIII wraps HRA and FP, while the HRB domain forms a trimer coiled spiral C-terminal connected to the transmembrane domain, followed by a short cytoplasmic tail. On receiving a signal from a homotypic attachment protein, the HRB uncoils and HRA projects the FP onto the target cell membrane to closely approach and finally merging of the two membranes. This process seems to describe

only the anchoring of the transmembrane domain, but it goes far beyond that.

In the current study, we obtained nine amino acids with similar properties by aligning the TM domain sequences of the four viruses, replaced them with alanine, which was changed to the corresponding T residues at A500 of the hPIV3 F protein, in order to illustrate its effect on fusion promotion. It is clear that certain amino acids are of great importance for its structure and function. Among them, A500T, I505A, V513A, V516A, L519A, and V520A possess reduced or undetectable capacities for the mediation of membrane fusion, and the inability of two sites substitutions (519 and 520) which were fusogenically active. Alternatively, the rest of the constructs performed to an equal extent compared with wild F in fusion promotion.

The abolished capabilities to fuse cells of mutants L519A and V520A were found to be strongly associated with low expression at the cell surface, as observed in IIFA and FACS. Moreover, confirmation that mutant F proteins do not properly traffic to the cell surface came from not identifying F_0 and F_1 bands in the subsequent cleavage activity experiments. In the case of the general cycle of membrane proteins, they are initially synthesized as peptides in ribosomes, then folded and glycosylated in the endoplasmic reticulum, from where they are transported to the Golgi apparatus for cutting, and are finally secreted on the cell surface. Intracellular transport along the secretory pathway goes hand in hand with sorting of proteins and lipids (19). Hence, a possible role for 519 and 520 residues without expression and fusion activity is not recognized in the cellular transport and sorting machinery (20,21). These residues have an impact on localization of the protein in the compartment where their function is required. There are, of course, protein-specific constraints on TM domain sequences imposed by the interactions and function of a particular protein (22). Leucine and valine, hydrophobic residues in the TM domain proximal position of the cytoplasmic tails, may be conserved amino acids in this region. An alternative possibility is that defective conformation owing to mutation is neither properly identified by the corresponding antibody nor has fusing accessibility.

V513A and V516A showed decreased fusion activity, possibly because they affected the TM-TM effect. Among the 20 naturally occurring amino acids, proline, glycine, and alanine have a structurally unique feature that helps to explain their low or high helix propensities (23). The incorporation of some β -branched amino acids are deemed to facilitate textural plasticity to membrane α -helices, which may be essential to protein function for lipid disorders and subsequent steps in membrane fusion (24,25). Substituting alanine for them gives rise to stronger interactions favorable to stable prefusion conformation (11) but deleterious to the follow-up protein function due to structural

rigidity (24). In a prevailing lipid-centric model of the fusion process, the attaching fusion peptide and transmembrane domain can concertedly act together on local membrane curvature to enhance pore opening, leading to lipid disorder, and spontaneous fusion (26). This has justified that fusion peptides derived from PIV5 and transmembrane domains can closely or loosely interact with homologous transmembrane domains to form thermodynamically advantageous coils in the lipid phase (8,27). This report is reminiscent of pivotal interaction between the FP and the TM domain of HIV gp41 (12). When V513 and V516 were mutated to alanine, the effect between the FP and the TM domain became weakened, resulting in the continuous expansion of fusion pores, manifested as content mixing and syncytium reduction. It is generally believed that β -strand conformation correlates with negative Gaussian curvature (NGC) (6), and that this curvature generation is geometrically necessary for topological changes during membrane remodeling in biological processes such as virus budding and membrane scission (28), while isoleucine and valine also have an inherent preference for β -strands (29), plus V513 and V516 are perhaps located in the core of the α -helix in the TM domain. Mutating the two together to alanine (or adding I510) may result in more failed fusion activity than a single mutation (not done in this study). In aggregate, these reasons may explain why V513A and V516A reduce fusion activity.

The construction A500T made the hypofusogenic mutant F protein, as observed in reporter gene assays (Figure 3B) and elucidated in syncytium assays (Figures 3C and 3D), where it was seen that the mutants caused 50% of wt F fusion levels. The residues that flank the hydrophobic membrane-spanning segments of membrane proteins might interact with the membrane-water interface, and strongly depend on specific properties of its amino acid side chains, including charge, hydrophobicity, polarity and potential for H-bonding (30). A500 could be located at the junction of the protein and the membrane. Fusion decline could be accounted for by a polarity change (from A to T), which may turn the interaction of the membrane-water interface, thus affecting its role. It was found that mutations within the membrane-proximal ectodomain region (MPER) of PIV5 (rich in serine and threonine) show both stabilizing and destabilizing activity (less fusion or increased fusion compared with wt F, respectively), suggesting that the MPER is a highly sensitive region of the protein (31). A500 is directly coupled to the MPER, so it might regulate fusion activity.

The fusion activity of construct I505A was decreased, as shown in previous experiment. In integral membrane proteins, tryptophan tends to locate at the membrane headgroup region, whereas isoleucine and alanine have a greater propensity to interact with the acyl chain region (30,32,33). I675A in MPER of HIV-1 gp41 may therefore

block the infectivity of cell-free virions by diminishing stabilizing interactions with the acyl chain region of the envelope, which predicted subtle changes in interfacial binding energy and hydrophobic moment (34). Likewise, the lower fusion activity of I505A is likely related to attenuated interactions with the acyl chain region, and thus adding to the mutation does not easily produce the negative curvature required for fusion.

In summary, the mutations we introduced into the TM domain of the NDV F exhibited various degrees of activity in membrane fusion, and the mutants A500T, I505A, V513A and V516A in this region altered the fusion function in BHK-21 cells. Sites L519 and V520 are crucial for F's production or architecture. This study of the F protein will provide supplementary data to further clarify the roles of this region in regulating membrane fusion activity.

Acknowledgements

We sincerely thank Dr. Bernard Moss of the National Institutes of Health for the wt and recombinant vaccinia virus vTF7-3 and Dr. Ronald M. Iorio of the University of Massachusetts Medical School for providing the recombinant plasmid vectors. Thanks to Dr. Edward C. Mignot, Shandong University, for linguistic advice.

Funding: This work was supported by grants from the National Natural Science Foundation of China (No. 81702814, No.81672011) and the Fundamental Research Funds of Shandong University (2015JC044).

Conflict of Interest: The authors have no conflicts of interest to disclose.

References

- Harrison SC. Viral membrane fusion. *Virology*. 2015; 479-480:498-507.
- Dutch RE, Hagglund RN, Nagel MA, Paterson RG, Lamb RA. Paramyxovirus fusion (F) protein: a conformational change on cleavage activation. *Virology*. 2001; 281:138-150.
- Lamb RA, Parks GD. Paramyxoviridae: The viruses and their replication. In: *Fields Virology* (Knipe DM, Howley PM, eds.). Wolters Kluwer/Lippincott Williams & Wilkins, Philadelphia, PA, USA, 2007; pp. 1449-1496.
- Harrison SC. Viral membrane fusion. *Nat Struct Mol Biol*. 2008; 15:690-698.
- Lee M, Yao HW, Kwon B, Waring AJ, Ruchala P, Singh C, Hong M. Conformation and trimer association of the transmembrane domain of the parainfluenza virus fusion protein in lipid bilayers from solid-state NMR: Insights into the sequence determinants of trimer structure and fusion activity. *J Mol Biol*. 2018; 430:695-709.
- Yao HW, Lee MW, Waring AJ, Wong GCL, Hong M. Viral fusion protein transmembrane domain adopts beta-strand structure to facilitate membrane topological changes for virus-cell fusion. *Proc Natl Acad Sci U S A*. 2015; 112:10926-10931.
- Smith EC, Culler MR, Hellman LM, Fried MG, Creamer TP, Dutch RE. Beyond anchoring: the expanding role of the hendra virus fusion protein transmembrane domain in protein folding, stability, and function. *J Virol*. 2012; 86:3003-3013.
- Donald JE, Zhang Y, Fiorin G, Carnevale V, Slochower DR, Gai F, Klein ML, DeGrado WF. Transmembrane orientation and possible role of the fusogenic peptide from parainfluenza virus 5 (PIV5) in promoting fusion. *Proc Natl Acad Sci U S A*. 2011; 108:3958-3963.
- Smith EC, Smith SE, Carter JR, Webb SR, Gibson KM, Hellman LM, Fried MG, Dutch RE. Trimeric transmembrane domain interactions in paramyxovirus fusion proteins: roles in protein folding, stability, and function. *J Biol Chem*. 2013; 288:35726-35735.
- Webb SR, Smith SE, Fried MG, Dutch RE. Transmembrane domains of highly pathogenic viral fusion proteins exhibit trimeric association *in vitro*. *mSphere*. 2018; 3:e00047-18.
- Barrett CT, Webb SR, Dutch RE. A hydrophobic target: Using the paramyxovirus fusion protein transmembrane domain to modulate fusion protein stability. *J Virol*. 2019; 93:e00863-19.
- Reuven EM, Dadon Y, Viard M, Manukovsky N, Blumenthal R, Shai Y. HIV-1 gp41 transmembrane domain interacts with the fusion peptide: implication in lipid mixing and inhibition of virus-cell fusion. *Biochemistry*. 2012; 51:2867-2878.
- Webb S, Nagy T, Moseley H, Fried M, Dutch R. Hendra virus fusion protein transmembrane domain contributes to pre-fusion protein stability. *J Biol Chem*. 2017; 292:5685-5694.
- Branttie JM, Dutch RE. Parainfluenza virus 5 fusion protein maintains pre-fusion stability but not fusogenic activity following mutation of a transmembrane leucine/isoleucine domain. *J Gen Virol*. 2020; 101:467-472.
- Gravel KA, McGinnes LW, Reitter J, Morrison TG. The transmembrane domain sequence affects the structure and function of the Newcastle disease virus fusion protein. *J Virol*. 2011; 85:3486-3497.
- Bissonnette MLZ, Donald JE, DeGrado WF, Jardetzky TS, Lamb RA. Functional analysis of the transmembrane domain in paramyxovirus F protein-mediated membrane fusion. *J Mol Biol*. 2009; 386:14-36.
- Liu Y, Chi MM, Wen HL, Zhao L, Song YY, Liu N, Chi LL, Wang ZY. The DI-DII linker of human parainfluenza virus type 3 fusion protein is critical for the virus. *Virus Genes*. 2020; 56:37-48.
- Welch BD, Liu YY, Kors CA, Leser GP, Jardetzky TS, Lamb RA. Structure of the cleavage-activated prefusion form of the parainfluenza virus 5 fusion protein. *Proc Natl Acad Sci U S A*. 2012; 109:16672-16677.
- Welch LG, Munro S. A tale of short tails, through thick and thin: investigating the sorting mechanisms of Golgi enzymes. *Febs Lett*. 2019; 593:2452-2465.
- Perrin J, Bary A, Vernay A, Cosson P. Role of the HIV-1 envelope transmembrane domain in intracellular sorting. *Bmc Cell Biol*. 2018; 19:3.
- Singh S, Mittal A. Transmembrane domain lengths serve as signatures of organismal complexity and viral transport mechanisms. *Sci Rep-Uk*. 2016; 6:22352.
- Sharpe HJ, Stevens TJ, Munro S. A comprehensive comparison of transmembrane domains reveals organelle-specific properties. *Cell*. 2010; 142:158-169.
- Blaber M, Zhang XJ, Matthews BW. Structural basis

- of amino-acid alpha-helix propensity. *Science*. 1993; 260:1637-1640.
24. Langosch D, Arkin IT. Interaction and conformational dynamics of membrane-spanning protein helices. *Protein Sci*. 2009; 18:1343-1358.
 25. Ollesch J, Poschner BC, Nikolaus J, Hofmann MW, Herrmann A, Gerwert K, Langosch D. Secondary structure and distribution of fusogenic LV-peptides in lipid membranes. *Eur Biophys J Biophys*. 2008; 37:435-445.
 26. Kozlov MM, McMahon HT, Chernomordik LV. Protein-driven membrane stresses in fusion and fission. *Trends Biochem Sci*. 2010; 35:699-706.
 27. Yao HW, Lee M, Liao SY, Hong M. Solid-state nuclear magnetic resonance investigation of the structural topology and lipid interactions of a viral fusion protein chimera containing the fusion peptide and transmembrane domain. *Biochemistry-US*. 2016; 55:6787-6800.
 28. Schmidt NW, Lis M, Zhao K, Lai GH, Alexandrova AN, Tew GN, Wong GCL. Molecular basis for nanoscopic membrane curvature generation from quantum mechanical models and synthetic transporter sequences. *J Am Chem Soc*. 2012; 134:19207-19216.
 29. Li SC, Deber CM. Glycine and beta-branched residues support and modulate peptide helicity in membrane environments. *FEBS Lett*. 1992; 311:217-220.
 30. Killian JA, von Heijne G. How proteins adapt to a membrane-water interface. *Trends Biochem Sci*. 2000; 25:429-434.
 31. Zokarkar A, Lamb RA. The paramyxovirus fusion protein C-terminal region: Mutagenesis indicates an indivisible protein unit. *J Virol*. 2012; 86:2600-2609.
 32. Senes A, Chadi DC, Law PB, Walters RFS, Nanda V, DeGrado WF. E-z, a depth-dependent potential for assessing the energies of insertion of amino acid side-chains into membranes: Derivation and applications to determining the orientation of transmembrane and interfacial helices. *J Mol Biol*. 2007; 366:436-448.
 33. Ulmschneider MB, Sansom MSP. Amino acid distributions in integral membrane protein structures. *BBA-Biomembranes*. 2001; 1512:1-14.
 34. Narasimhulu VGS, Bellamy-McIntyre AK, Laumaea AE, Lay CS, Harrison DN, King HAD, Drummer HE, Pombourios P. Distinct functions for the membrane-proximal ectodomain region (MPER) of HIV-1 gp41 in cell-free and cell-cell viral transmission and cell-cell fusion. *J Biol Chem*. 2018; 293:6099-6120.

Received September 1, 2020; Revised December 4, 2020; Accepted January 21, 2021.

**Address correspondence to:*

Liyang Wang, Department of Clinical Laboratory, Qilu Hospital, Cheeloo College of Medicine, Shandong University, Ji'nan, Shandong Province, 250012, China.
E-mail: wangliyang@sdu.edu.cn

Zhiyu Wang, Department of Virology, School of Public Health, Cheeloo College of Medicine, Shandong University, Ji'nan 250012, Shandong Province, China.
E-mail: zhiyu.wang@sdu.edu.cn

Released online in J-STAGE as advance publication January 27, 2021.